JOURNAL OF AMASYA UNIVERSITY THE INSTITUTE OF SCIENCES AND TECHNOLOGY (JAUIST)

A STUDY ON THE FREQUENCY RESPONSE OF A COMPOSITE PRE-STRESSED SYSTEM UNDER AN INCLINED HARMONIC LOADING

Ahmet DAŞDEMİR

Department of Mathematics, Faculty of Sciences, Kastamonu University, Kastamonu/Turkey
ORCID: https://orcid.org/0000-0001-8352-2020

Research Type: Research article
Received: 04/08/2022, Accepted: 10/12/2022
*Corresponding author: ahmetdasdemir37@gmail.com

Abstract

Goal for the present research is investigating the dynamic behaviors regarding forced vibration of an elastic composite body on the rigid ground for four different material designations. For this purpose, the effects of the initial stress state and frequency response parameter on the forced vibration of the model are studied. Based on the linearized theory of elasticity, the nonlinear forced vibration of composite material on the rigid ground is considered. The nonlinear governing equations are linearized and boundary-contact conditions are derived using Hamilton's principle. Total energy functional is constructed based on the principle of the variational formulation, and then the forced vibration of elastic composite plate-strip is analyzed using the finite element method (FEM). Moreover, the numerical examples related to the influences of important problem factors on our mathematical model are given. The observations show that the selection of more soft material in the upper layers has a great potential for the structural stability of the system. For the softer upper layer relatively, the wave oscillation in the plate-strip exhibits becomes more regular. In addition, the resonance values of the system decrease with the increase of the initial compressing parameter but with the initial stretching parameter.

Key Words: Composite material, Initial stress, Finite element method, Frequency response, Forced vibration.

Özet

Bu araştırmanın amacı, dört farklı malzeme tasarımına sahip rijit zemin üzerindeki elastik bir kompozit cismin zorlanmış titreşimine ilişkin dinamik davranışları araştırılmaktır. Bu amaçla, modelin zorlanmış titreşimi üzerindeki ilk gerilme durumu ve frekans tepkisi parametresinin etkileri incelenmiştir. Lineerleştirilmiş elastisite teorisine dayalı olarak, rijit zemin üzerindeki kompozit malzemenin lineer olmayan zorlanmış titreşimi göz önünde bulundurulmuştur. Doğrusal olmayan alan denklemleri doğrusallaştırılmış ve Hamilton ilkesi kullanılarak sınır-temas koşulları türetimiştir. Toplam enerji fonksiyoneli, varyasyonel formülasyon ilkesine dayalı olarak oluşturulurmuştur ve daha sonra, sonlu elemanlar yöntemi (FEM) kullanılarak elastik kompozit plaka-şeritin zorlanmış titreşimi analiz edilmiştir. Ayrıca önemli problem faktörlerinin matematiksel modelimize etkileri ile ilgili sayısal örnekler verilmiştir. Gözlemler, üst katmanlarda daha yumuşak malzeme seçiminin sistemin yapısal kararlılığı için büyük bir potansiyele sahip olduğunu göstermektedir. Nispeten daha yumuşak üst tabaka için, plaka-şerit sergilerindeki dalga salınımı daha düzenli hale gelir. Ayrıca sistemin rezonans değerleri, artan ilk sıkıştırma parametresi ve ilk gerilme parametresi ile azalmaktadır.

Anahtar Kelimeler: Kompozit malzeme, Başlangıç gerilmesi, Sonlu eleman metodu, Frekans tepkisi, Zorlanmış titreşim

1. Introduction

The general elasticity theory for homogeneous materials has been under the density study by several investigators. To solve the corresponding problems, many systematic theories and solution procedure are presented due to different requirements. The dynamic response of the multilayered elastic materials is affected significantly by many external factors. According to recent developments, the static pre-stressed case in the body which exist before the additional

dynamical force becomes increasingly important. These initial stresses in the considered body may arise for the reason such that a technological process or the environmental temperature. It is impossible to analyze the influence of the pre-stressed states within the scope of the well-known linear theory of elasticity since the mentioned influence is non-linear. On the other hand, when the value of the external dynamic impact applied to the material is considerably less than the one of the initial loading, the relevant problems can be made with respect to the linearized theory of elastic waves in bodies under initial stress. Note that this theory was created within the scope of elastodynamics. The fundamental monographs by Guz (1999) and Akbarov (2015) provides extensive information on the subject.

There are many studies dedicated to the considerations of wave propagation in solids with initial stretching or systems containing such bodies today. Abo-el-Nour et al. (2009) reported an analysis of the effect of initial stresses the propagation of acoustic surface waves in a piezoelectric cylinder covered with an elastic layer. Wang et al. (2010) considered the influence of the flexural wave propagating along a nano-plate let in a pre-stressed elastic matrix. Abd-Alla et al. (2011) searched the influence of the gravity field on the speediness of the propagation of S-wave in an anisotropic incompressible pre-stretching environment. Güven (2012) presented a report regarding the propagation of longitudinal stress waves in a nano-bar in the existence of the initial stress case. Singh (2013) studied wave reflection and refraction at the interface of different configurations of a couple of piezoelectric and elastic materials. Farhan (2013) considered the velocity of Rayleigh waves along a pre-stretched infinite cylinder with thermal stress. Kundu et al. (2014) discussed oscillations of Love waves along fiber-reinforced anisotropic layer standing on an orthotropic half-plane numerically. Li and Tao (2015) studied the influence of the initial stress case on certain special types of wave propagation in a rock mass. Nam et al. (2016) investigated harmonic wave oscillations of infinitesimal magnitude waves in a layer resting on a half-plane with initial stress. Daşdemir (2017) considered the effect of the initial stress state in Elastic/Piezoelectric/Elastic composite materials with incomplete contact under a dynamic force. Biswas and Abo-Dahab (2018) solved a problem related to the propagations of Rayleigh surface waves in a thermoelastic material with initial stress according to the phase-lag model. Ejaz and Shams (2019) derived the dispersion relations related to the Love waves propagating along a compressible hyperelastic layer standing on a half-plane for which both bodies are having initial stresses. Sharma (2020) examined the influence of the initial stress case on the propagation of

Rayleigh waves along the surface of an orthotopic material gravitational environment. Babych and Glukhov (2021) considered a vibration problem by moving force at the top surface in a multi-layered half-plane with initial stresses. Panja and Mandal (2022) numerically solved the stress field problem related to several viscoelastic strips resting on a viscoelastic orthotropic half-plane with initial stresses by using the finite difference method. It should be noted that there exist mechanical reviews including many problems with different configurations, which we neglect here, in the current literature.

From the author's knowledge, the harmonical vibration problem in an elastic composite material with initial stresses under an inclined dynamic external force standing on a rigid ground has not been studied analytically so far, and there is a lack of a mathematical model to present a main approach for explaning the influence of the selection of materials. To dispose of this issue, a mathematical modeling to analyze the frequency response of the pre-stressed plate-strip is constituted. First, we derive linear governing equations and present appropriate boundary-contact conditions. Using the variational formulation technique, we create a finite element model for the problem. Next, we give numerical results regarding the configuration of the plate-strip.

2. Problem Formulation

Figure 1 displays the composite plate-strip of length $2a$ on rigid foundation. Each layer is elastic material of thickness h_i, where $i=1,2,3,4.$ We assume that the layers are perfectly clamped together, that each layer is homogeneous and isotropic, that there is no slipping at interfaces, and that the thickness of the clamping at the interfaces is omitted. Total thickness of the plate-strip is h, and $h=h_1+h_2+h_3+h_4$. The Cartesian coordinate system has its origin at the midpoint of the top boundary of the body; namely, the axes Ox_1 and Ox_2 are along the length and thickness directions, respectively. Summing up, the problem domain can be written as $B=B_1\cup B_2\cup B_3\cup B_4$, where

$$\begin{aligned}
B_1&=\left\{\left(x_1,x_2,x_3\right):-a\le x_1\le a,-h_1\le x_2\le 0,-\infty\le x_3\le\infty\right\},\\
B_2&=\left\{\left(x_1,x_2,x_3\right):-a\le x_1\le a,-h_1-h_2\le x_2\le -h_1,-\infty\le x_3\le\infty\right\},\\
B_3&=\left\{\left(x_1,x_2,x_3\right):-a\le x_1\le a,-h_1-h_2-h_3\le x_2\le -h_1-h_2,-\infty\le x_3\le\infty\right\},\\
B_4&=\left\{\left(x_1,x_2,x_3\right):-a\le x_1\le a,-h\le x_2\le -h_1-h_2-h_3,-\infty\le x_3\le\infty\right\}.
\end{aligned}\tag{2.1}$$

Note that the layer materials are the linear elastic, homogenous and isotropic. For an elastic medium, the constitutive equations can be expressed as

$$\sigma_{ij}^{(m)} = \lambda^{(m)} \varepsilon_{\ell\ell}^{(m)} \delta_{ij} + 2\mu^{(m)} \varepsilon_{ij}^{(m)}, \quad \varepsilon_{ij}^{(m)} = \left(u_{i,j}^{(m)} + u_{j,i}^{(m)} \right) / 2 \tag{2.2}$$

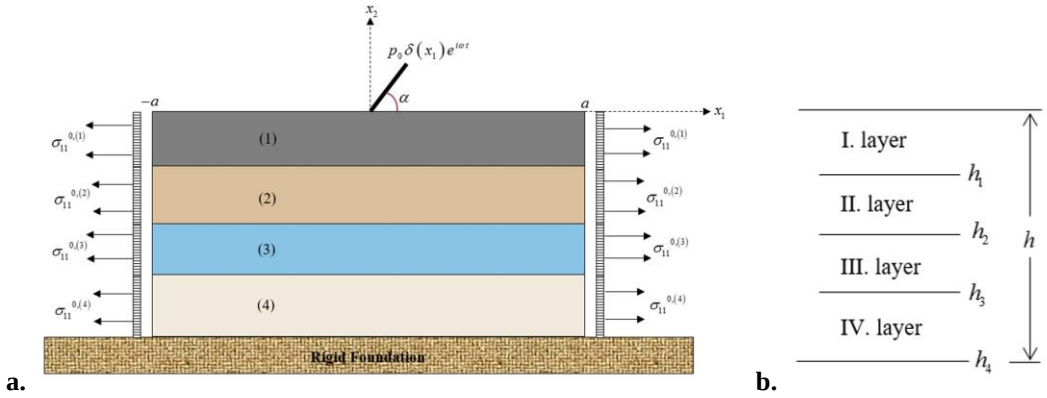

a. **b.**

Figure 1. (a) Elastic composite layered structure and (b) Scheme of layers

where $u_i^{(m)}$ and $\sigma_{ij}^{(m)}$ are the corresponding displacement and stress components, $\lambda^{(m)}$ and $\mu^{(m)}$ are the Lamé parameters, δ_{ij} is the Kronecker's delta function, and $\varepsilon_{ij}^{(m)}$ are the strain components.

While constructing the body, the lateral sides of each layer are first subjected to a uniaxial homogeneous static force. Note that each initial stress state has a different magnitude. Following this, four layers are compounded to create the pre-stressed body and left on a rigid ground. Following, a time-harmonic dynamic loading is applied to the resultant system such that the amplitudes of the dynamical perturbations are considerably less than the static state's ones.

The initial stresses in the above-stated are determined by utilizing the linear theory of elasticity as follows:

$$\sigma_{11}^{(m),0} = q^{(m)}, \text{ and } \sigma_{ij}^{(m),0} = 0 \text{ for other cases,} \tag{2.3}$$

where $m = 1, 2, 3, 4$ and $q^{(m)}$ is the constant initial stress value for the corresponding layer.

As seen from the above, the width of each layer is, in fact, infinite along the axis Ox_3. However, the dynamic force is also extending to infinity in this direction. Hence, the plane deformation state occurs on the plane Ox_1x_2. This allows us to make all the next research on this plane. In addition, the superscript "*(m)*" indicates the quantity related to the corresponding layer, and the subscript "0" to the initial case.

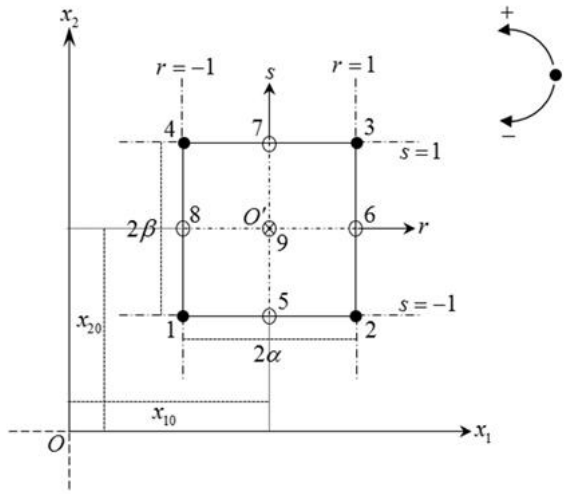

Figure 2. A typical finite element and the order of nodes

Considering the above assumptions and the general bases of the classical theory of elasticity, nonlinear governing equations of motion can be expressed as

$$\frac{\partial}{\partial x_i'}\left[\sigma_{ik}^{(m)}\left(\delta_{kj}+\frac{\partial u_j^{(m)}}{\partial x_k'}\right)\right]=\rho^{(m)}\frac{\partial^2 u_i^{(m)}}{\partial t^2}, \tag{2.4}$$

where t is the time-parameter and $\rho^{(m)}$ is the mass density of the mth layer. By the way, in the initial case, Eq. (2.4) is written as

$$\frac{\partial}{\partial x_i'}\left[\sigma_{ik}^{(m),0}\left(\delta_{kj}+\frac{\partial u_j^{(m),0}}{\partial x_k'}\right)\right]=0\,. \tag{2.5}$$

In addition, due to the external harmonic force varying with the time , all the components such as displacement or stress can be discretized as $[\square]^{(m)}=[\hat{\square}]^{(m)}e^{i\omega t}$, where $i=\sqrt{-1}$, and e is famous

Euler constant. For readability, we omit the hats over quantities after this. After this discretization, Eq. (2.4) can be arranged as

$$\frac{\partial}{\partial x_i'}\left[\sigma_{ik}^{(m)}\left(\delta_{kj}+\frac{\partial u_j^{(m)}}{\partial x_k'}\right)\right]+\rho^{(m)}\omega^2\tilde{u}_i^{(m)}=0 \tag{2.6}$$

Substituting the perturbations $\sigma_{ik}^{(m)}=\tilde{\sigma}_{ik}^{(m)}+\tilde{\sigma}_{ik}^{(m),0}$ and $u_j^{(m)}\cong\tilde{u}_j^{(m)}+\tilde{u}_j^{(m),0}$ into Eq. (2.6) yields

$$\frac{\partial}{\partial x_i'}\left[\left\{\tilde{\sigma}_{ik}^{(m)}+\tilde{\sigma}_{ik}^{(m),0}\frac{\partial\tilde{u}_j^{(m)}}{\partial x_k'}\right\}+\left\{\tilde{\sigma}_{ik}^{(m)}\frac{\partial\tilde{u}_j^{(m)}}{\partial x_k'}+\tilde{\sigma}_{ik}^{(m),0}\frac{\partial\tilde{u}_j^{(m),0}}{\partial x_k'}+\tilde{\sigma}_{ik}^{(m)}\frac{\partial\tilde{u}_j^{(m),0}}{\partial x_k'}\right\}\right] \tag{2.7}$$
$$+\rho^{(m)}\omega^2\tilde{u}_i^{(m)}=0$$

All the terms in the second parenthesis of the above equation can be neglected and $\tilde{\sigma}_{ik}^{(m),0}$ is a constant. After the coordinate transformation $\tilde{x}_i=x_i/h$, the following equations of motion are reached:

$$\sigma_{ij,j}^{(m)}+\sigma_{11}^{(m),0}u_{i,11}^{(m)}+\rho^{(m)}\omega^2h^2u_i^{(m)}=0 \tag{2.8}$$

Here and below, we ignore the upper tilde over the quantities. Also, the repeated index in the subscript means summation protocol with respect to that index and the subscripts after the commas denote partial derivative with respect to the corresponding coordinates.

Further, the following boundary-contact terms are held:

$$\sigma_{21}^{(1)}\Big|_{x_2=0}=-p_0\delta(x_1)\mathrm{e}^{\mathrm{i}\omega t}\cos\alpha\,,\ \sigma_{22}^{(1)}\Big|_{x_2=0}=-p_0\delta(x_1)\mathrm{e}^{\mathrm{i}\omega t}\sin\alpha\,, \tag{2.9}$$

$$\sigma_{i2}^{(1)}\Big|_{x_2=-h_1/h}=\sigma_{i2}^{(2)}\Big|_{x_2=-h_1/h},\ u_i^{(1)}\Big|_{x_2=-h_1/h}=u_i^{(2)}\Big|_{x_2=-h_1/h}, \tag{2.10}$$

$$\sigma_{i2}^{(2)}\Big|_{x_2=(-h_1-h_2)/h}=\sigma_{i2}^{(3)}\Big|_{x_2=(-h_1-h_2)/h},\ u_i^{(2)}\Big|_{x_2=(-h_1-h_2)/h}=u_i^{(3)}\Big|_{x_2=(-h_1-h_2)/h}, \tag{2.11}$$

$$\sigma_{i2}^{(3)}\Big|_{x_2=(-h_1-h_2-h_3)/h}=\sigma_{i2}^{(4)}\Big|_{x_2=(-h_1-h_2-h_3)/h},\ u_i^{(3)}\Big|_{x_2=(-h_1-h_2-h_3)/h}=u_i^{(4)}\Big|_{x_2=(-h_1-h_2-h_3)/h}, \tag{2.12}$$

$$\left(\sigma_0^{(m)}u_{j,1}^{(m)}+\sigma_{1j}^{(m)}\right)\Big|_{x_1/h=\pm a/h}=0\,, \tag{2.13}$$

$$u_j^{(4)}\Big|_{x_2=-1}=0\,, \tag{2.14}$$

where $\delta(\cdot)$ is the Dirac's famous function. Here, the boundary conditions in Eq. (2.9) is mechanical traction-free conditions because of the dynamic force, Eqs. (2.10)-(2.12) are complete contact

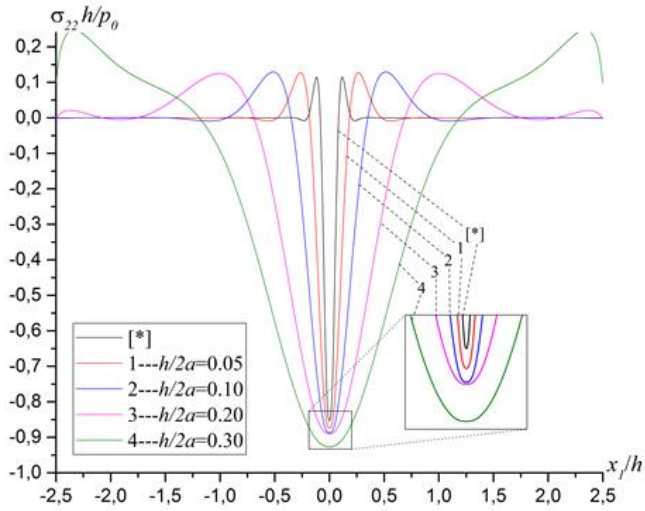

Figure 3. The graphs of $\sigma_{22}h/p_0$ versus x_1/h for various thickness ratio under the same assumption in the paper of Uflyand (1963)

interaction terms at the interfaces, Eq. (2.13) is mechanically open conditions, and Eq. (2.14) is mechanically free conditions by the rigid foundation. Hence, this completes the statement of our model.

3. Solution Method

In this study, we employ the Finite Element Method (FEM) to obtain an approximate solution for the present problem according to the virtual work law. (Zienkiewicz and Taylor, 1989)

We first consider the open form of the system of partial equations in Eq. (2.8). Each equation is summed after multiplying the test functions $v_i = v_i(x_1, x_2)$. By the way, these are not random functions and satisfy governing equations in Eq. (2.8) and the boundary-contact conditions in Eqs. (2.9)-(2.14). We integrate the resultant equation over the domain B, apply the main principles of the variational formulation and obtain the following functional after wide mathematical arrangements:

$$J\left(\mathbf{u}^{(m)}\right)=\frac{1}{2}\iint_{B}\left\{\begin{array}{l}\left(\frac{c_1^{(m)}}{c_2^{(m)}}\right)^2\left[\left(\frac{\partial u_1^{(m)}}{\partial x_1}\right)^2+\left(\frac{\partial u_2^{(m)}}{\partial x_2}\right)^2\right]+2\frac{\lambda^{(m)}}{\mu^{(m)}}\frac{\partial u_1^{(m)}}{\partial x_1}\frac{\partial u_2^{(m)}}{\partial x_2}+\left[\frac{\partial u_1^{(m)}}{\partial x_2}+\frac{\partial u_2^{(m)}}{\partial x_1}\right]^2\\ +\eta^{(m)}\left[\left(\frac{\partial u_1^{(m)}}{\partial x_1}\right)^2+\left(\frac{\partial u_2^{(m)}}{\partial x_1}\right)^2\right]-\left(\Omega^{(m)}\right)^2\left[\left(u_1^{(m)}\right)^2+\left(u_1^{(m)}\right)^2\right]\end{array}\right\}dA \\ +\int_{-a/h}^{a/h}p_0\frac{\delta(x_1)}{\mu^{(1)}}\left(u_1^{(1)}\cos\alpha+u_2^{(1)}\sin\alpha\right)\Big|_{x_2=0}dx_1. \qquad (3.1)$$

where

$$c_1^{(m)}=\sqrt{\lambda^{(m)}+2\mu^{(m)}/\rho^{(m)}},\ c_2^{(m)}=\sqrt{\mu^{(m)}/\rho^{(m)}},\ \Omega^{(m)}=\frac{\omega h}{c_2^{(m)}},\ \text{and}\ \eta^{(m)}=\sigma_0^{(m)}/\mu^{(m)}. \qquad (3.2)$$

In Eq. (3.2), $c_1^{(m)}$ and $c_2^{(m)}$ represent the velocity of dilatation waves and the distortion wave, and $\Omega^{(m)}$ and $\eta_2^{(m)}$ are the dimensionless frequency and the initial stress parameters, respectively.

The reliability of the functional presented in (2.12) is shown as follows. Using Gauss' theorem and computing the first variation of Eq. (3.1) such as $\delta J\left(\mathbf{u}^{(m)}\right)=0$, we get our equations and the related terms that construct the problem, completing the desired proof.

Considering Eq. (3.1), we can define the representations

$$\mathbf{P}=\frac{1}{2}\iint_{B}\left\{\begin{array}{l}\left(\frac{c_1^{(m)}}{c_2^{(m)}}\right)^2\left[\left(\frac{\partial u_1^{(m)}}{\partial x_1}\right)^2+\left(\frac{\partial u_2^{(m)}}{\partial x_2}\right)^2\right]+2\frac{\lambda^{(m)}}{\mu^{(m)}}\frac{\partial u_1^{(m)}}{\partial x_1}\frac{\partial u_2^{(m)}}{\partial x_2}+\left[\frac{\partial u_1^{(m)}}{\partial x_2}+\frac{\partial u_2^{(m)}}{\partial x_1}\right]^2\\ +\eta^{(m)}\left[\left(\frac{\partial u_1^{(m)}}{\partial x_1}\right)^2+\left(\frac{\partial u_2^{(m)}}{\partial x_1}\right)^2\right]\end{array}\right\}dA$$

$$\mathbf{K}=\frac{1}{2}\iint_{B}\left(\Omega^{(m)}\right)^2\left[\left(u_1^{(m)}\right)^2+\left(u_1^{(m)}\right)^2\right]dA,\ \text{and}\ \mathbf{Z}=\int_{-a/h}^{a/h}p_0\frac{\delta(x_1)}{\mu^{(1)}}\left(u_1^{(1)}\cos\alpha+u_2^{(1)}\sin\alpha\right)\Big|_{x_2=0}dx_1.$$

Based on Hamilton's principle, the total strain energy of composite plate-strip can be expressed as:

$$\delta\left(\mathbf{P}-\omega^2\mathbf{K}-\mathbf{Z}\right)=0, \qquad (3.3)$$

where $\mathbf{P}$, $\mathbf{K}$, and $\mathbf{Z}$ are the potential, kinetic, and virtual loading energies, respectively.

For developing the finite element model of Eq. (3.1), we can apply the well-known Rayleigh-Ritz method on the basis of the virtual work principle. (Zienkiewicz and Taylor, 1989) We first discretize the problem domain into more subdomains and select a master subdomain. Next, we

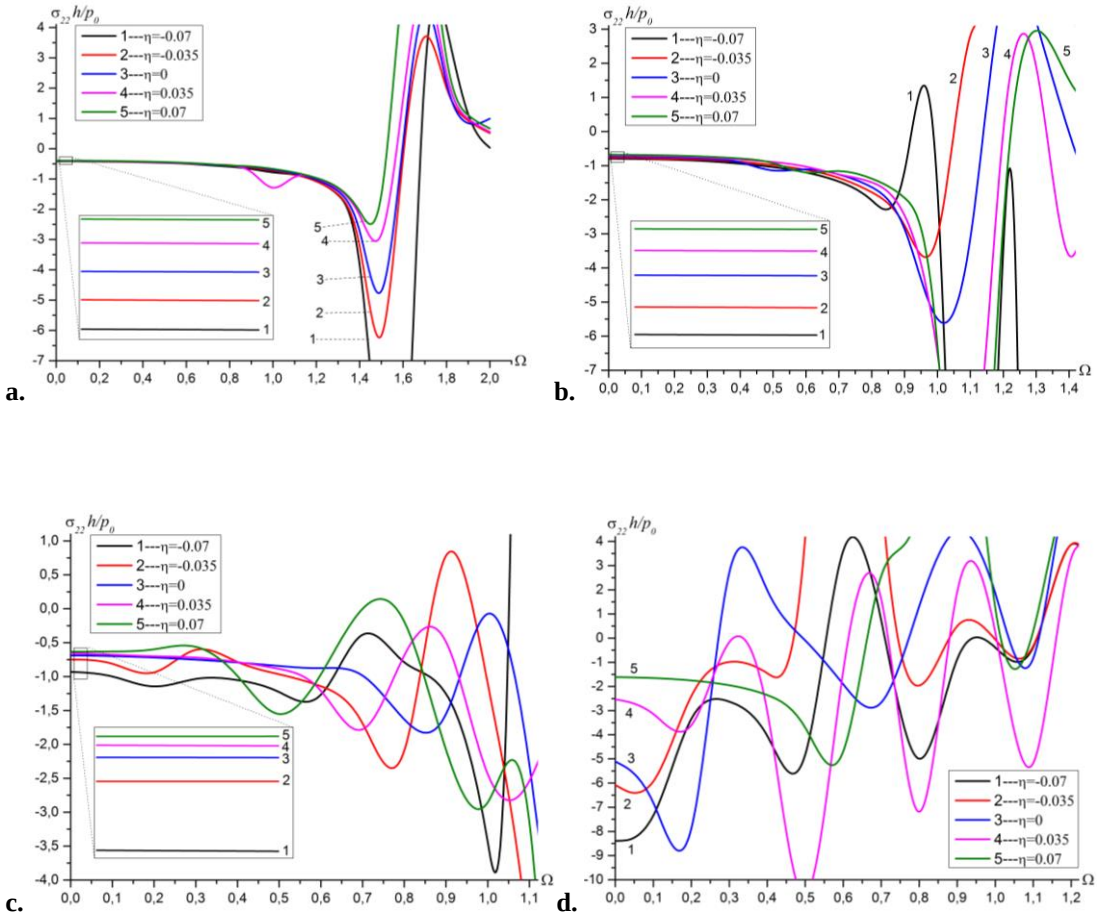

Figure 4. The stress $\sigma_{22}h/p_0$ versus Ω for various η and $\alpha=\pi/2$ under (a) Case I, (b) Case II, (c) Case III, and (d) Case IV

mark nine nodes over the master element, as shown in Fig. 2. Therefore, the displacement functions can be written as $u_1^{(k)}=\sum_{i=1}^{9}a_i^{(k)}N_i(r,s)$ and $u_2^{(k)}=\sum_{i=1}^{9}b_i^{(k)}N_i(r,s)$, (3.4)

where a_i and b_i are the unknown coefficients, r and s are normalized coordinates, and $N_j(r,s)$ represents the shape functions defined over the domain $[-1,1]\times[-1,1]$. The explicit forms of the used shape functions are as follows: (Hutton, 2004)

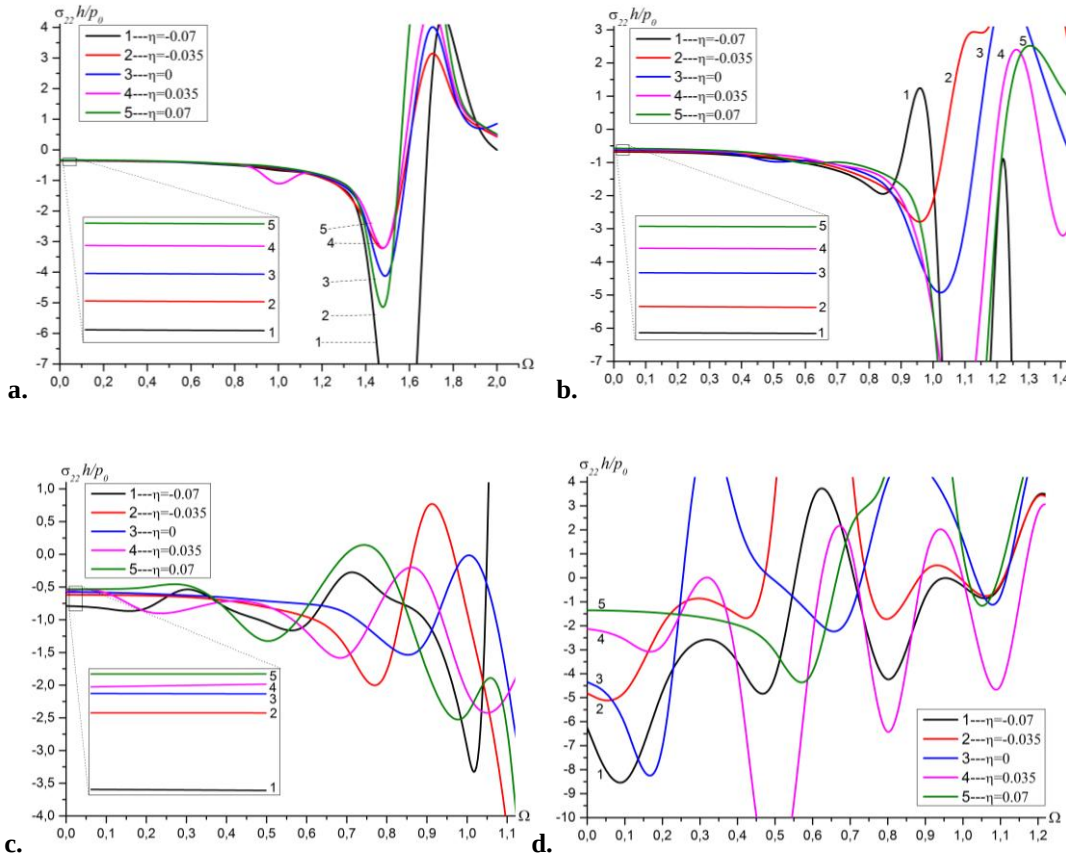

Figure 5. The stress $\sigma_{22}h/p_0$ versus Ω for various η and $\alpha=\pi/3$ under (a) Case I, (b) Case II, (c) Case III, and (d) Case IV

$$N_1(r,s)=\frac{1}{4}(r^2-r)(s^2-s),\ N_2(r,s)=\frac{1}{4}(r^2+r)(s^2-s),\ N_3(r,s)=\frac{1}{4}(r^2+r)(s^2+s),$$
$$N_4(r,s)=\frac{1}{4}(r^2-r)(s^2+s),\ N_5(r,s)=-\frac{1}{2}(r^2-1)(s^2-s),\ N_6(r,s)=-\frac{1}{2}(r^2+r)(s^2-1),$$
$$N_7(r,s)=-\frac{1}{2}(r^2-1)(s^2+s),\ N_8(r,s)=-\frac{1}{2}(r^2-r)(s^2-1),\ N_9(r,s)=(r^2-1)(s^2-1).$$

In this situation, the displacements obtained the nodes can be ordered as follows:

$$\mathbf{u}_m=\begin{bmatrix}\mathbf{u}_{m1} & \mathbf{u}_{m2}\end{bmatrix}^T=\begin{bmatrix}u_{11} & u_{12} & \dots & u_{18} & | & u_{21} & u_{22} & \dots & u_{28}\end{bmatrix}^T$$

Substituting Eq. (3.4) into the total strain energy functional in Eq. (3.3), then using the Rayleigh-Ritz method (Zienkiewicz and Taylor, 1989), the following matrix-vector system can be obtained:

$$\left(\mathbf{K}\text{-}\omega^2\mathbf{M}\right)\tilde{\mathbf{u}} = \mathbf{F}\,, \tag{3.5}$$

where $\mathbf{K}$ and $\mathbf{M}$ are the stiffness and mass matrices, and $\tilde{\mathbf{u}}$ and $\mathbf{F}$ are the displacement and force vector. Since the matrices in Eq. (3.5) are symmetric, real, and positive definite, we can obtain a unique solution to find the corresponding displacement values. Hence, we can compute the required stress values to be able to make the numerical investigations.

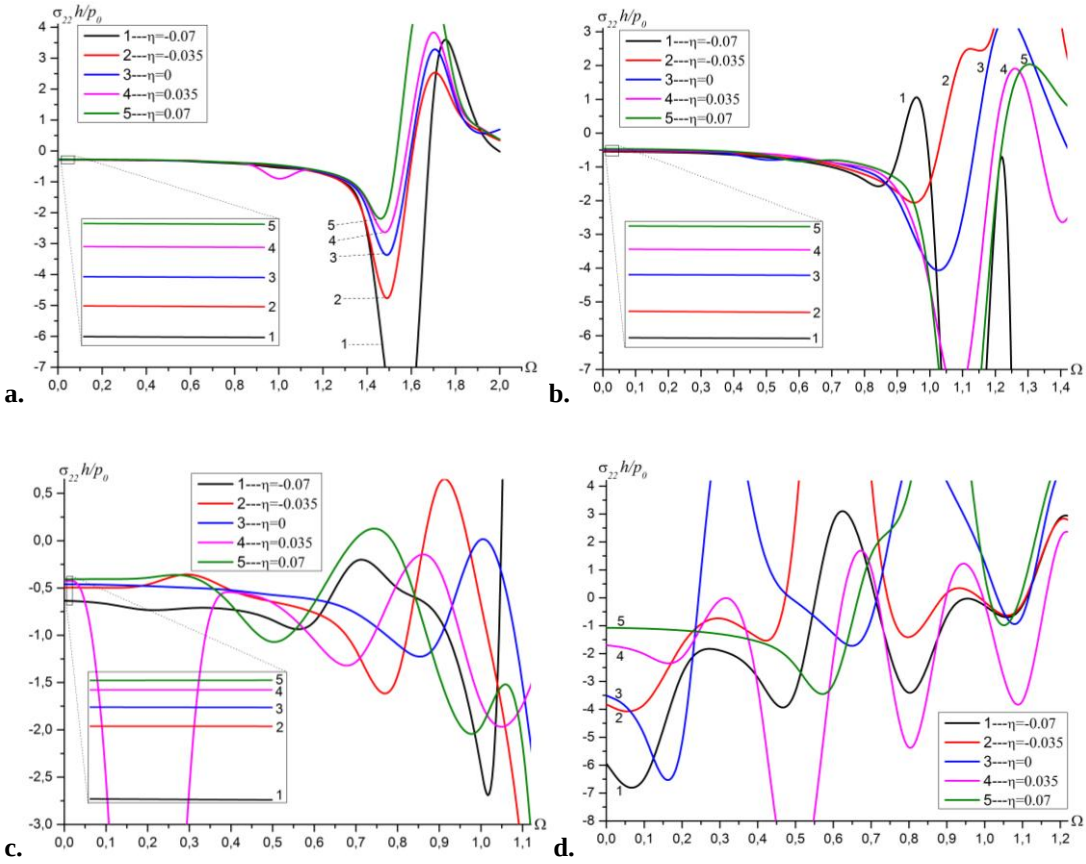

Figure 6. The stress $\sigma_{22}h/p_0$ versus Ω for various η and $\alpha = \pi/4$ under (a) Case I, (b) Case II, (c) Case III, and (d) Case IV

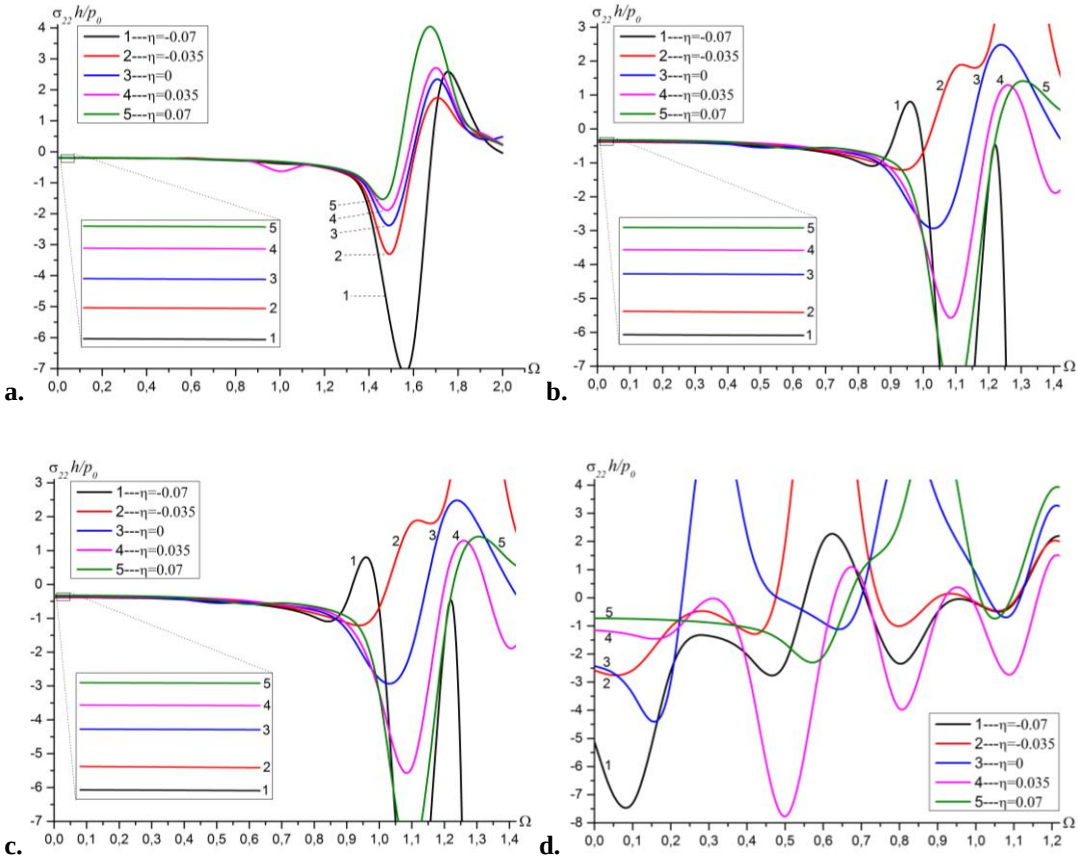

Figure 7. The stress $\sigma_{22}h/p_0$ versus Ω for various η and $\alpha=\pi/6$ under (a) Case I, (b) Case II, (c) Case III, and (d) Case IV

4. Results and Discussion

The number of the rectangular finite elements in the horizontal and vertical directions are 200 and 25, respectively. Hence, for the present FEM modelling, 40902 NDOFs are identified in total. Note that the used materials are selected as Aluminum (shortly Al) with properties $\nu^{(Al)}=0.35$ and $\rho^{(Al)}=2.7\times10^3\ \ kg/m^3$ and Steel (shortly St) with properties $\nu^{(St)}=0.29$ and $\rho^{(Al)}=7.86\times10^3\ \ kg/m^3$. Throughout the numerical investigations, the case wherein $h/2a=0.2$, $h_1=h_2=h_3=h_4$, $\Omega^{(1)}=\Omega^{(2)}=\Omega^{(3)}=\Omega^{(4)}=\Omega$, $\eta^{(1)}=\eta^{(2)}=\eta^{(3)}=\eta^{(4)}=\eta$, $\Omega=0$, and $\eta=0$ is considered unless otherwise specified. Moreover, four different cases are considered as follows:

Case I: Al+Al+St+St, Case II: St+Al+Al+St, Case III: Al+St+St+Al, and Case IV: St+St+Al+Al. It should be noted that all the graphs are given at the point where $\left(x_1 / h, x_2 / h\right) = \left(0, -1\right)$.

Before the numerical results, the validity and trustiness of computer algorithm developed for the current problem must be proven. To do this, the case where $h / 2a \to \infty$ is considered. In this case, the scheme of the problem becomes the similar to that investigated by Uflyand (1963). Hence the numerical results must converge to these given by Uflyand (1963) under the same assumptions. This forecasting is approved by Fig. 3. It should be noted that the starred graph in Fig. 3 indicates that of Uflyand (1963). Consequently, the proof is shown. In addition, increasing values of the ratio $h / 2a$ lead to decrease the absolute values of the normal stress $\sigma_{22} h / p_0$. Note that graph marked by asterisk is the result of Uflyand (1963).

Figs. 4-7 show the effect of the inclined force on the frequency behavior of the system for Cases I-IV. Moreover, under drawing of the graphs various values of η are considered. The absolute values of $\sigma_{22} h / p_0$ decrease as the initial compressing increases but as the initial stretching decrease. At the same time, An increase in the angle of the force leads also to attain the larger values of the stress $\sigma_{22} h / p_0$. It is seen from the graphs in Figs. 4-7, the most stable choice of the considered system is under Case I. It follows from Figs. 4-7 that there exist certain places where the normal stress has a maximum value for some values of Ω. These are called as "resonance value" (represented by Ω^*). Increasing values of the initial compressing leads to decrease the resonance values of the plate-strip but the initial stretching parameter to increase these values. The mentioned values decrease with the selection of from Case I to Case IV. Furthermore, increasing values of the angle of the force leads to decrease the resonance values of the considered body. Also the numerical findings show that there exist the parametric resonance values of $\sigma_{22} h / p_0$ in the certain values of η based on the selection of the considered cases. For example, in Fig. 4a the distribution of $\sigma_{22} h / p_0$ is temporarily unstable in the range of $0.9 \le \Omega \le 1.1$ in the case where $\eta = 0.035$. Similarly, the comparison of Fig. 6b and Fig. 7b indicate that the region where the distribution of $\sigma_{22} h / p_0$ is temporarily unstable change with the selection of the materials in the case where $\eta = 0.070$.

4. Conclusion

Based on the three-dimensional linearized theory of elastic waves in initially stressed bodies (TLTEWISB), the forced vibration of elastic composite plate-strip on the rigid foundation is studied in this paper. Using Hamilton's principle, the nonlinear governing equations are linearized and the related boundary-contact conditions are given. The fundamental principle of the variational formulation is applied to the partial differential equations, and then the forced vibration of plate-strip is numerically analyzed using the finite element method (FEM). The results show that the selection of more soft material in the upper layers can enhance the structural stability of the system. With the increase of the initial compressing parameter, the resonance values of the plate-strip tend to decrease. On the contrary, increasing values of the initial stretching parameter cause to increase these resonance values. In addition, the numerical findings show that there exist the parametric resonance values of $\sigma_{22}h / p_0$ for certain values of η.

Conflicts of interest

The authors declare that there are no potential conflicts of interest relevant to this article.

References

Abo-el-Nour, N., Al-sheikh, F., & Al-Hossain, A. Y. (2009). Effect of initial stresses on dispersion relation of transverse waves in a piezoelectric layered cylinder. Materials Science and Engineering: B, 162(3), 147-154.

Abd-Alla, A. M., Mahmoud, S. R., Abo-Dahab, S. M., & Helmy, M. I. (2011). Propagation of S-wave in a non-homogeneous anisotropic incompressible and initially stressed medium under influence of gravity field. Applied Mathematics and Computation, 217(9), 4321-4332.

Akbarov, S. D. (2015). Dynamics of pre-strained bi-material elastic systems: Linearized three-dimensional approach. Springer, New York, NY, USA.

Babych, S. Y., & Glukhov, Y. P. (2021). On One Dynamic Problem for a Multilayer Half-Space with Initial Stresses. International Applied Mechanics, 57(1), 43-52.

Biswas, S., & Abo-Dahab, S. (2018). Effect of phase-lags on Rayleigh wave propagation in initially stressed magneto-thermoelastic orthotropic medium. Applied Mathematical Modelling, 59, 713-727.

Daşdemir, A. (2017). Effect of imperfect bonding on the dynamic response of a pre-stressed sandwich plate-strip with elastic layers and a piezoelectric core. Acta Mechanica Solida Sinica, 30(6), 658-667.

Ejaz, K., & Shams, M. (2019). Love waves in compressible elastic materials with a homogeneous initial stress. Mathematics and Mechanics of Solids, 24(8), 2576-2590.

Farhan, A. M. (2013). Effect of Initial Stress on Wave Propagation in an Infinite Generalized Thermoelastic Circular Cylinder. Journal of Computational and Theoretical Nanoscience, 10(9), 2269-2275.

Guz, A. N. (1999). Fundamentals of the three-dimensional theory of stability of deformable bodies. Springer, New York, NY, USA. [Translated from Russian by M. Kashtalian.]

Güven, U. (2012). A more general investigation for the longitudinal stress waves in microrods with initial stress. Acta Mechanica, 223(9), 2065-2074.

Hutton, D. (2004). *Fundamentals of Finite Element Analysis*. McGraw-Hills, New York, 2004

Kundu, S., Gupta, S., & Manna, S. (2014). Propagation of Love wave in fiber‐reinforced medium lying over an initially stressed orthotropic half‐space. International Journal for Numerical and Analytical Methods in Geomechanics, 38(11), 1172-1182.

Li, X., & Tao, M. (2015). The influence of initial stress on wave propagation and dynamic elastic coefficients. Geomechanics & Engineering, 8(3), 377-390.

Nam, N. T., Merodio, J., Ogden, R. W., & Vinh, P. C. (2016). The effect of initial stress on the propagation of surface waves in a layered half-space. International Journal of Solids and Structures, 88, 88-100.

Panja, S. K., & Mandal, S. C. (2022). Propagation of Love wave in multilayered viscoelastic orthotropic medium with initial stress. Waves in Random and Complex Media, 32(2), 1000-1017.

Sharma, M. D. (2020). Propagation of Rayleigh waves at the boundary of an orthotropic elastic solid: Influence of initial stress and gravity. Journal of Vibration and Control, 26(21-22), 2070-2080.

Singh, B. (2013). Rayleigh wave in an initially stressed transversely isotropic dissipative half-space. Journal of Solid Mechanics, 5(3), 270-277.

Uflyand, Y. S. (1963). *Integral Transformations in the Theory of Elasticity*, Nauka, Moscow-Leningrad, 1963

Wang, Y. Z., Li, F. M., & Kishimoto, K. (2010). Scale effects on flexural wave propagation in nanoplate embedded in elastic matrix with initial stress. Applied Physics A, 99(4), 907-911.

Zienkiewicz O. C., & R. L. Taylor, R. L. (1989). *The Finite Element Method, Basic Formulation and Linear Problems*, vol. 1 (4th ed.), McGraw-Hill, London.